The Development of SOL Transport Model for Integrated Core-SOL Simulation of *L*-mode Plasma

A. Wisitsorasak[1,2], T. Onjun[3] and B. Chatthong[4]

[1]Department of Physics, Faculty of Science, King Mongkut's University of Technology Thonburi, Bangkok, Thailand
[2]Theoretical and Computational Science Center (TaCS), Faculty of Science, King Mongkut's University of Technology Thonburi, Bangkok, Thailand
[3]School of Manufacturing Systems and Mechanical Engineering, Sirindhorn International Institute of Technology, Thammasat University, Pathum Thani, Thailand
[4]Department of Physics, Faculty of Science, Prince of Songkla University, Songkla, Thailand

Corresponding Author: apiwat.wis@kmutt.ac.th

Abstract:
Simulations of the plasma in the core and scrape-off layer (SOL) regions are carried out using 1.5D BALDUR integrated predictive modeling code in low confinement mode (*L*-mode). In each simulation, the plasma current, temperatures, and density profiles in both core and SOL regions are evolved self-consistency. The plasma profiles in the SOL region are simulated by integrating the fluid equations, including sources, along the field lines. The solutions in the SOL subsequently provide as the boundary conditions of the core plasma region. The core plasma transport model is described using a combination of anomalous transport by Multi-Mode-Model version 1995 (MMM95) and neoclassical transport provided by NCLASS module. Furthermore, the calculation of the toroidal velocity used in this work is based on the torque due to intrinsic neoclassical toroidal viscosity (NTV). While the transport coefficients in the SOL region are either determined by either a fixed constant or neoclassical transport based on NCLASS calculation. By comparing with 38 *L*-mode discharges from TFTR, DIII-D, and JET, It is found that the average RMS deviations of the SOL transport modeled by the neoclassical theory are 16.8% for the electron density, 14.0% for the electron temperature, and 19.8% for the ion temperature, while the simulation results using the SOL transport modeled with a fixed constant show more deviation. Thus SOL transport modeled by the neoclassical theory yields better agreement with the experimental data than that using a fixed constant.

1 Introduction

All man-made plasmas are produced in machine of finite size and always involve interaction with solid matters at reactor walls. The dynamics of plasma in the boundary

layer that forms a transition zone between the hot and magnetically confined plasma and material walls also differs from the dynamics of the core plasma and is still under active research. In the past few years, a large number of transport models in the core and scrape-off layer (SOL) regions have been developed to predict the plasma plasma profiles in tokamak [1]. The objective of this work is to investigate the transport models of the plasma in the scrape-off layer (SOL) in which it provides a necessary boundary condition for the plasma transport in the core region. In this study, we compare the simulation results which are modeled by two different scenarios of the SOL transport coefficients: (A) the transport coefficients that solely determined from the neoclassical transport and (B) constant transport coefficients which are in order of the Bohm coefficients [2].

2 Description of Codes

In this work, we employ 1.5D BALDUR integrated predictive modeling code to self-consistently simulate the plasma in both core and scrape-off layer (SOL) for L-mode tokamak operation [3, 4, 5]. For core transport model, NCLASS module is used to calculate the neoclassical transport of multi-species axisymmetric plasma of arbitrary aspect ratio, geometry and collisionality, while the anomalous transport is simulated by the Multi-Mode Model version 1995 (MMM95). MMM95 is a theory-motivated transport model and consists of the Weiland model for the ion temperature gradient (ITG) and trapped electron mode (TEM), the Guzdar-Drake model for drift-resistive ballooning modes, and kinetic ballooning mode. The expressions of the transport coefficient in MMM95 can be given as

$$\chi_i = 0.8\chi_{i,ITG\&TEM} + 1.0\chi_{i,RB} + 0.65\chi_{i,KB}, \quad (1)$$

$$\chi_e = 0.8\chi_{e,ITG\&TEM} + 1.0\chi_{e,RB} + 0.65\chi_{e,KB}, \quad (2)$$

$$D_H = 0.8D_{H,ITG\&TEM} + 1.0D_{H,RB} + 1.0D_{H,KB}, \quad (3)$$

$$D_Z = 0.8D_{Z,ITG\&TEM} + 1.0D_{Z,RB} + 1.0D_{Z,KB}, \quad (4)$$

where χ_e is the electron diffusivity, χ_i is the ion diffusivity, D_H is the hydrogenic particle diffusivity, D_Z is the impurity diffusivity, $\chi_{ITG\&TEM}$ is the thermal diffusivity of ion temperature gradient and trapped electron mode, χ_{RB} is the resistive ballooning thermal diffusivity, and χ_{KB} is the kinetic ballooning thermal diffusivity. All the anomalous transport contributions to MMM95 transport model were derived for circular plasmas. It was found that multiplying such transport contributions by the inverse fourth power of the local elongation of plasma produced the observed scaling of confinement time [6].

The plasma entering the SOL region also flows along the opened magnetic field lines until it reaches the neutralizer plate. Consequently, the resulting neutral gas interacts with the incoming plasma and modifies its properties and flow dynamics. The main effect in this region is a large recycling of the neutral gas in which the neutrals are ionized by the plasma near the edge and are swept back to the neutralizer. The cycle repeatedly occurs through the whole operation of a tokamak. This dynamics serves to amplify the particle flux and reduce the temperature, thereby minimizing erosion. The amplification

of the particle flux, in turn, reduces the upstream plasma flow velocity along the field lines in the SOL region, thus modifying the edge density of the main plasma region.

In the SOL region, we have used the sheath model to describe the plasma flow to the divertor [7]. The divertor plate is assumed to be an insulated conductor, with no net current flow. The density and energy in the SOL region can be described using the diffusion equation including the loss term corresponding to particle and energy flows to the divertor. A tokamak can also be approximated as a long cylinder. For the tokamak with a poloidal divertor, a field line must travel around the torus about $q(a)$ times from the divertor plate before encountering it again. Thus the average path length (L) of the particle that travel along magnetic field lines in this region can be written as $L = \pi R\, q(a)$. For the ions, the continuity equation reads

$$\frac{\partial n}{\partial t} = \nabla \cdot (D_\perp \nabla n) - \frac{n v_s}{L} + S_n, \tag{5}$$

where v_s is the ion sound speed ($v_s = ((T_e + T_i)/m_i)^{1/2}$), S_n is the particle source, and $D_\perp$ is the diffusion coefficient across the field lines. The transport coefficients in the SOL region are normally found to be lower than those in the core area and approximately equal to about 10% of the Bohm values [8]. In this work we compare the transport coefficients in two cases. For case A, the transport coefficients are solely determined from the neoclassical transport, but not the anomalous transport as accounted for the plasma in the core area (this case will be referred as *model A*). For case B, the coefficients are constants with predefined values and can be described as: $D_i^{SOL} = \chi_i^{SOL} = 0.5\chi_e^{SOL} = 0.25$ m$^2\cdot$ s^{-1} [2] (this case will be hereinafter referred as *model B*).

The neoclassical transport is carried out in BALDUR code using NCLASS module [9]. The module accounts for the neoclassical effects which refer to the flows resulting from Coulomb collisions between particles drifting in non-uniform magnetic and electric fields. NCLASS module calculates the neoclassical transport properties of a multi-species axisymmetric plasma of arbitrary aspect ratio, geometry and collisionality. It determines a multi-fluid model for the parallel and radial force balance equations which consequently lead to the neoclassical bootstrap current, parallel electrical resistivity, impurity and fuel ion radial particle transport, ion radial thermal transport and plasma poloidal rotation.

3 Simulation Results and Discussion

The plasma profiles are predicted using the anomalous core transport model (MMM95) to couple with the SOL model for 38 discharges from TFTR, DIII-D, and JET tokamaks. All discharges were in the *L*-mode regime and were heated with NBI. The simulated profile are then validated with the experimental data which are available in Ref. [10]. Table I provides a list of all discharges that were investigated in this study. Discharge numbers 1-32 were obtained from TFTR tokamak, while discharge numbers 33 - 36 and 37 - 38 were taken from DIII-D and JET tokamaks respectively. For all simulations, The boundary conditions for densities and temperatures at the edge of the plasma are respectively set to 1 eV and 10^{17} m^{-3} [11].

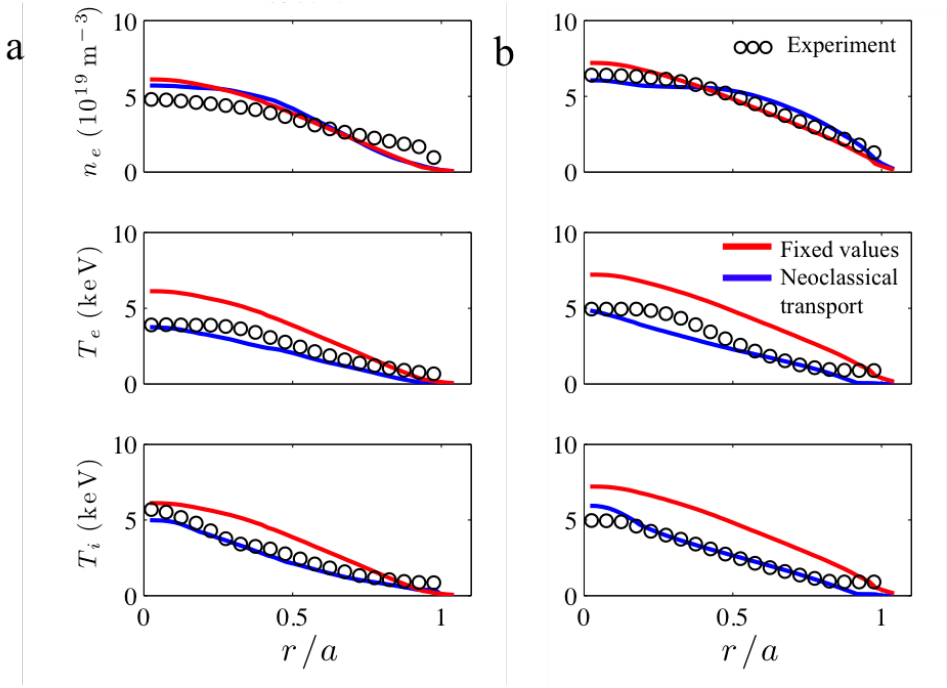

FIG. 1: Simulated plasma profiles compared with the experimental data for (a) TFTR#45980 and (b) JET#19649.

3.1 Profile Comparison

Figure 1 shows two samples of the simulated profiles of electron density and electron and ion temperatures for (a) TFTR#45980 and (b) JET#19649 discharges. The simulations with the SOL transport with fixed values of the transport coefficient (model B) match the experimental results poorly. Especially the core transports for both discharges of TFTR and JET show lack of fit. These observations will be then quantitatively confirmed by the statistical analysis which will be discussed in the next section.

3.2 Statistical Analysis

To quantify the comparison between the simulations and experiments for the 38 L-mode discharges, the percentage of root-mean-square (RMS) deviations is computed as followed

$$\mathrm{RMS} \equiv \sqrt{\frac{1}{N}\sum_{i=1}^{N}\left(\frac{x_{sim,i}-x_{exp,i}}{x_{exp,max}}\right)^2} \times 100, \tag{6}$$

where $x_{exp,i}$ is the i^{th} data point of the experimental profiles, $x_{sim,i}$ is the corresponding value from the simulated profile, and N is the total number of data points [4]. The relative offset of each quantity x ($x \in \{n_e, T_e, T_i\}$) which compares the simulation prediction and

the experimental data is defined as

$$\text{OFFSET} \equiv \frac{1}{N}\sum_{i=1}^{N}\left(\frac{x_{sim,i}-x_{exp,i}}{x_{exp,max}}\right). \tag{7}$$

A positive offset indicates that the simulated profile is predominantly higher than the experimental data, and vice versa.

The statistical analysis is then conducted to compare the SOL transport models with the experimental results. Figure 2 presents the RMS deviation of the simulated profiles of the electron density, electron and ion temperatures which are predicted by the models for each discharge. The blue bars represent the simulation results predicted by SOL transport determined solely by the neoclassical transport (model A), while the red bars are the results predicted by SOL transport with predefined values (model B). As seen in this figure, the RMS deviations of model A for the electron density, electron and ion temperature are lower than those of model B.

The average relative offset and RMS deviation of all discharges are illustrated in figure 3. It can be seen in figure 3a that both SOL transport models (model A and B) under predict the electron density profile, while transport model B over predicts the temperature profiles. This observation also reflects in the average RMS deviation in figure 3b. Thus the statistical analysis draw a conclusion that the SOL transport using model A tends to agree with the experimental data more than those using the SOL transport with model B.

4 Conclusion

In this study of 38 *L*-mode discharges in TFTR, DIII-D, and JET, the plasma in the core and the SOL regions are carried out using 1.5D BALDUR integrated predictive modeling code. The core transport is determined by using a combination of anomalous transport (MMM95) and the neoclassical theory, while the SOL transport is predicted using 2 models: (A) the neoclassical transport, and (B) the predefined values with fixed constants which are described as $D_i^{SOL} = \chi_i^{SOL} = 0.5\chi_e^{SOL} = 0.25$ m$^2\cdot$ s^{-1} [2]. Quantitative assessments of the two models are based on the relative offset and RMS deviation. It is found that the average RMS of model A are 16.8% for the electron density, 14.0% for the electron temperature, and 19.8% for the ion temperature, while the average RMS of model B are 18.5%, 48.6%, and 48.4% for the electron density, electron and ion temperatures, respectively. Thus the SOL transport modeled by the neoclassical theory yields better agreement with the experimental data.

Acknowledgements

This work is part of a collaborative research project under the Center of Plasma and Nuclear Fusion Technology (CPaF) and was supported by the Theoretical and Computational Science (TaCS) Center under Computational and Applied Science for Smart Innovation Research Cluster (CLASSIC), Faculty of Science, KMUTT.

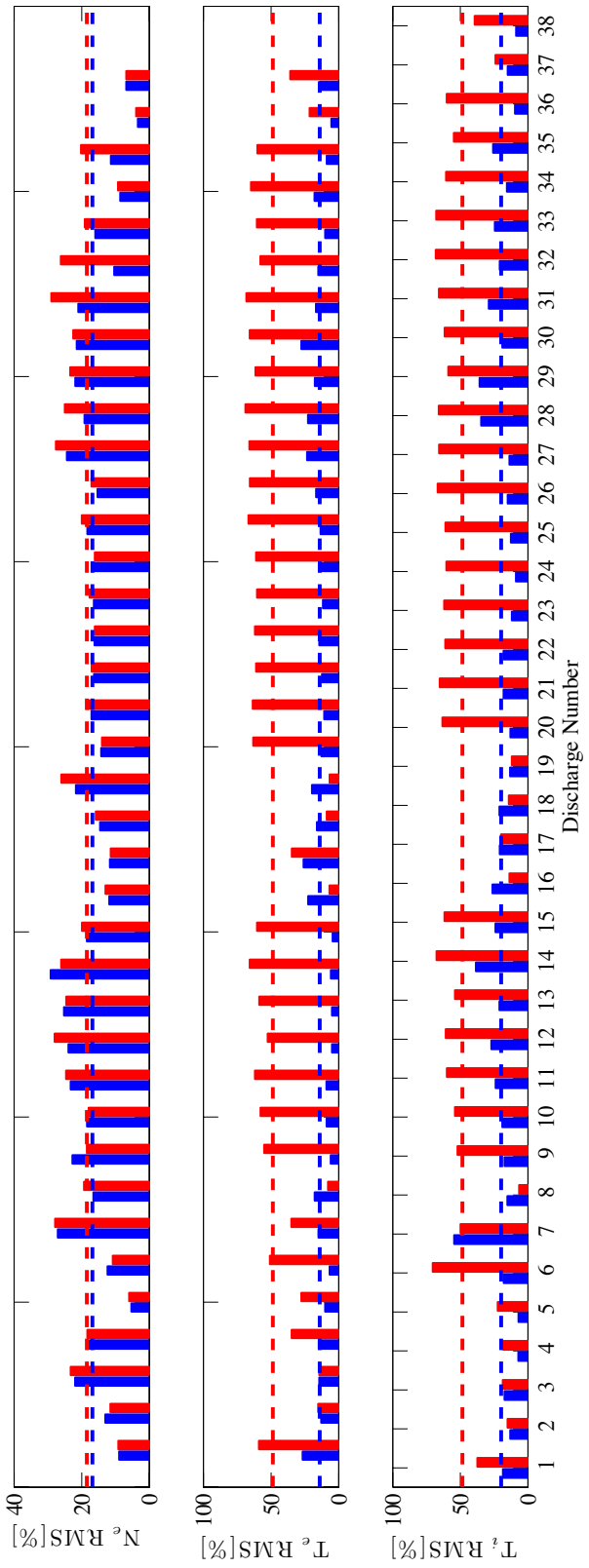

FIG. 2: Plots of the RMS deviations of the electron density (N_e), electron temperature (T_e), and ion temperature (T_i) for the 38 L-mode discharges. Please see table I for the shot ID of each discharge number.

TABLE I: List of plasma discharges with engineering parameters. Note that discharge numbers 1-32 were obtained from TFTR, numbers 33 - 36 from DIII-D, and numbers 37 - 38 from JET.

No.	Shot ID	R (m)	a (m)	κ	δ	B_T (T)	I_P (MA)	$\bar{n}_e$ (10^{19} m^{-3})	$\bar{Z}_{eff}$	P_{aux} (MW)	t_{diag} (s)
1	45359	2.58	0.93	1.00	0.01	3.75	1.79	4.65	2.90	4.52	4.41
2	45950	2.46	0.80	1.04	0.01	4.79	2.00	3.30	2.95	11.40	4.54
3	45966	2.46	0.80	1.02	0.02	4.76	1.00	3.30	2.52	11.39	4.58
4	45980	2.45	0.80	0.96	0.02	4.77	0.99	3.35	2.84	11.33	4.89
5	45984	2.45	0.80	0.92	0.01	4.78	0.98	3.51	2.43	11.25	4.12
6	46290	2.52	0.86	1.04	0.02	4.65	2.00	4.22	3.09	11.19	4.59
7	46291	2.52	0.86	1.04	0.02	4.65	2.00	4.27	3.18	11.20	4.55
8	52179	2.46	0.80	0.95	0.02	4.74	0.98	3.35	2.42	12.77	4.53
9	52182	2.46	0.81	0.93	0.01	4.75	0.94	4.67	2.15	10.49	3.94
10	52183	2.46	0.81	1.04	0.02	4.74	1.98	6.28	2.04	12.68	3.47
11	52184	2.46	0.81	0.93	0.01	4.75	0.96	6.02	1.85	12.71	3.93
12	52186	2.46	0.81	1.04	0.02	4.74	1.98	6.60	1.74	12.77	3.48
13	52187	2.46	0.81	1.04	0.02	4.74	1.98	6.61	2.06	12.69	3.46
14	52188	2.46	0.80	1.04	0.02	4.74	1.98	6.49	2.04	12.74	3.44
15	52194	2.46	0.81	1.04	0.02	4.74	1.98	7.11	1.53	12.73	3.45
16	52233	2.46	0.80	1.04	0.02	4.74	1.98	5.73	2.15	12.68	3.50
17	50904	2.45	0.80	1.00	0.01	2.86	1.19	2.73	2.05	7.31	3.95
18	50911	2.45	0.80	1.00	0.01	4.23	1.78	4.37	1.79	17.72	3.93
19	50921	2.45	0.80	1.00	0.01	2.14	0.89	1.77	2.24	4.66	3.95
20	105290	2.53	0.87	1.04	0.02	4.74	1.97	5.28	1.34	14.20	4.50
21	105294	2.52	0.87	1.04	4.00	4.76	1.97	5.20	1.62	13.82	4.50
22	105305	2.53	0.87	1.04	0.02	4.74	1.97	4.65	1.36	13.80	4.49
23	105310	2.53	0.87	1.04	0.02	4.74	1.97	5.23	1.21	11.50	4.49
24	105313	2.53	0.87	1.04	0.02	4.75	1.97	4.80	1.18	9.28	4.50
25	105314	2.53	0.87	1.04	0.02	4.74	1.97	5.25	1.17	11.69	4.50
26	105317	2.53	0.87	1.04	0.02	4.74	1.97	5.23	1.33	11.23	4.49
27	105324	2.53	0.87	1.04	0.02	4.74	1.97	5.25	1.17	11.91	4.49
28	105338	2.52	0.87	1.03	0.03	2.39	0.99	3.79	1.27	11.60	4.50
29	105340	2.52	0.87	1.02	0.02	2.39	0.99	4.17	1.12	11.85	4.49
30	105343	2.52	0.87	1.02	0.02	2.39	0.99	4.10	1.09	9.43	4.49
31	105352	2.52	0.87	1.03	0.03	2.39	0.99	4.43	1.17	11.31	4.50
32	105353	2.52	0.87	1.02	0.03	2.39	0.99	4.42	1.13	11.58	4.50
33	69627	1.66	0.64	1.70	0.12	1.01	1.01	3.90	2.00	3.30	2.40
34	69648	1.67	0.65	1.65	0.13	1.98	2.00	9.64	4.00	15.30	4.10
35	71378	1.62	0.60	1.52	0.23	1.01	0.70	3.68	2.00	3.50	2.98
36	71384	1.63	0.61	1.48	0.16	2.00	1.39	8.90	3.00	14.60	3.45
37	19649	2.97	1.16	1.43	0.03	3.12	3.05	3.49	2.16	9.11	48.65
38	19691	2.97	1.16	1.42	0.03	3.06	3.05	4.77	3.65	15.35	54.50

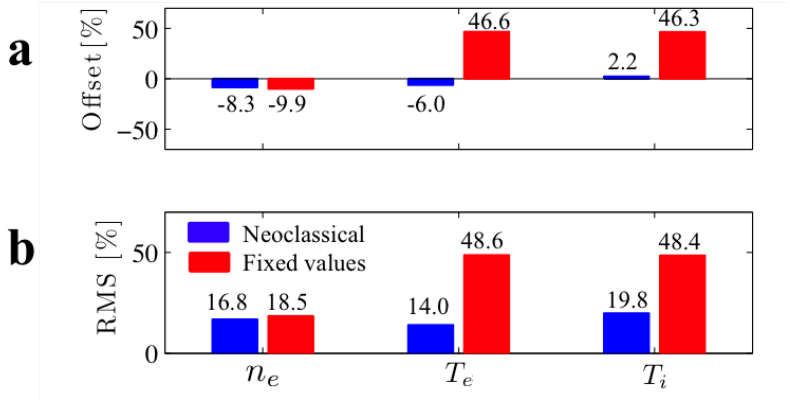

FIG. 3: The average relative offset and the average RMS deviation of the electron density (n_e), electron (T_e) and ion (T_i) temperatures of the 38 L-mode discharges.

References

[1] Stangeby, P. C. et al., *The plasma boundary of magnetic fusion devices*, volume 224, Institute of Physics Publishing Bristol, 2000.

[2] Zagórski, R., Ivanova-Stanik, R., and Stankiewicz, R., Nuclear Fusion **53** (2013) 073030.

[3] Singer, C. et al., Computer physics communications **49** (1988) 275.

[4] Onjun, T., Bateman, G., Kritz, A. H., and Hannum, D., Physics of Plasmas (1994-present) **8** (2001) 975.

[5] Bateman, G., Onjun, T., and Kritz, A. H., Plasma physics and controlled fusion **45** (2003) 1939.

[6] Bateman, G., Kritz, A. H., Kinsey, J. E., Redd, A. J., and Weiland, J., Physics of Plasmas (1994-present) **5** (1998) 1793.

[7] Hobbs, G. and Wesson, J., Plasma Physics **9** (1967) 85.

[8] Ogden, J., Post, D., Jensen, R., and Seidl, F., One-dimensional transport code modelling of the limiter-divertor region in tokamaks, Technical report, Princeton Univ., 1980.

[9] Houlberg, W., Shaing, K., Hirshman, S., and Zarnstorff, M., Physics of Plasmas (1994-present) **4** (1997) 3230.

[10] Boucher, D. et al., Nuclear fusion **40** (2000) 1955.

[11] Pianroj, Y. and Onjun, T., Songklanakarin Journal of Science & Technology **36** (2014).